Scientia Horticulturae xxx (xxxx) 114984

Contents lists available at ScienceDirect

Scientia Horticulturae

journal homepage: www.sciencedirect.com/journal/scientia-horticulturae

Research Paper

Integrated physiological and biochemical screening of commercial and novel grapevine rootstocks under drought stress

Sara Anichini[a], Giampiero Cai[b,*], Tommaso Betti[b], Marco Romi[b], Davide Bianchi[c], Lucio Brancadoro[c], Sara Parri[b]

[a] Department of Agriculture, Food, Environment and Forestry (DAGRI), University of Florence, Piazzale delle Cascine 18, 50144, Florence, Italy
[b] Department of Life-Sciences, University of Siena, Via Mattioli 4, 53100, Siena, Italy
[c] Department of Agricultural and Environmental Sciences (DiSAA)-Production, Landscape, Agroenergy, University of Milano, Via G. Celoria 2, 20133, Milan, Italy

ARTICLE INFO

Keywords:
Vitis spp.
Water deficit
Water use efficiency
Gas exchange
Antioxidants
Aquaporins
Osmotic adjustment

ABSTRACT

Climate change is increasing drought frequency and severity in Mediterranean viticulture, making drought-resilient rootstocks essential for future vineyard sustainability. This study used the Microcosmo controlled field simulator to compare six grapevine rootstock genotypes (161.49-C, Dog Ridge, cc114, cc125, cc136 and cc177) under progressive water deficit monitored by soil-moisture sensors. Drought reduced gas exchange rates in all genotypes, albeit with distinct patterns. Dog Ridge exhibited an initial sharp decline, while cc125, cc136 and 161.49-C displayed basal gas exchange maintenance. cc114 and cc177, on the other hand, exhibited linear decreases. Maximum PSII efficiency remained largely unaffected, whereas effective PSII efficiency and electron transport rate decreased mainly under severe drought. Biochemical profiling revealed contrasting adaptive strategies. Most genotypes increased superoxide dismutase, sucrose synthase and HSP70. cc125 showed the strongest coordinated activation of antioxidant, metabolic and protein-protection responses. Aquaporin accumulation was high in cc114 and cc136, but low in cc177, suggesting different hydraulic regulation strategies. Glucose and fructose accumulation supported osmotic adjustment in cc125 and cc114. In contrast, Dog Ridge exhibited sugar depletion, and cc136 failed to increase hexoses despite strong sucrose synthase induction. Markers of oxidative status, including antioxidant power, phenolic compounds, flavonoids and malondialdehyde, revealed that antioxidant activation does not necessarily prevent membrane lipid peroxidation. Overall, cc125 was the most promising non-commercial genotype, demonstrating high water-use efficiency, sustained photosynthetic performance, osmotic adjustment and strong stress-protein induction. cc114 exhibited a balanced response involving hydraulic regulation, flavonoid accumulation and moderate oxidative damage. In contrast, cc136 exhibited early photosynthetic activity but was susceptible to oxidative damage. These findings demonstrate that combining physiological, metabolic, protein and oxidative markers is an effective way of identifying novel grapevine rootstocks that are suited to Mediterranean viticulture in areas with limited water.

1. Introduction

The Mediterranean region is renowned for being one of the most suitable areas for viticulture, primarily thanks to its climate. Its warm, dry summers and cool, wet winters create ideal conditions for producing high-quality wines (Keller, 2010; Rogiers et al., 2022). However, this traditional advantage is under threat from the ongoing and accelerating effects of climate change. The combination of rising global temperatures and an increased frequency and intensity of extreme weather events, such as heatwaves and prolonged droughts, poses a significant challenge to the sustainability of viticulture in Mediterranean regions (Sucu et al., 2018; Ali et al., 2025).

One of the most critical consequences of climate change is the alteration of temperature and precipitation patterns. Projections suggest that regions suitable for viticulture may gradually shift towards higher latitudes and altitudes, encompassing areas that were previously deemed too cold for grape cultivation (Keller, 2010; Tomás et al., 2014; Van Leeuwen et al., 2019; Jones et al., 2022). Meanwhile, the Mediterranean region is experiencing increasingly severe water shortages due to reduced rainfall and falling groundwater levels (Van Leeuwen et al.,

* Corresponding author.
E-mail address: cai@unisi.it (G. Cai).

https://doi.org/10.1016/j.scienta.2026.114984
Received 30 January 2026; Received in revised form 23 May 2026; Accepted 22 June 2026
0304-4238/

2019). Although irrigation is often seen as a way of addressing water scarcity, it is not a sustainable long-term solution due to problems such as salinisation, aquifer depletion and competition for water resources (Marusig and Tombesi, 2020). Furthermore, elevated temperatures can affect the phenology of grapevines, accelerating developmental stages and potentially altering the composition of the fruit. Changes in sugar accumulation, acidity and aromatic profiles can significantly affect wine quality, which has economic and cultural implications for regions where viticulture is deeply rooted (Ali et al., 2025).

Vitis vinifera L. was selected for this study because it is a valuable perennial crop cultivated in over 90 countries for wine production and table grapes (Rius-Garcia, 2025). The Mediterranean region is particularly important, accounting for around 39% of the world's vineyard area, covering approximately 7.3 million hectares (Rius-Garcia, 2025). However, in this area, viticulture is under threat from soil salinization and drought, both of which are major causes of desertification (Cuena Lombraña et al., 2022; Rius-Garcia, 2025). Drought stress significantly impacts productivity and is estimated to cause annual crop yield losses of 65–87% globally. Specifically, water deficit can significantly increase the rate of flower abscission in sensitive cultivars, thereby reducing the quality and yield of grapes (Scholasch and Rienth, 2019). As over 80% of global vineyards utilize *Vitis vinifera* grafted onto rootstocks, it is crucial to understand the physiological and molecular mechanisms of drought resilience in order to develop sustainable viticultural strategies for arid and semi-arid regions (Bianchi, 2023). The way in which grapevines adapt to a lack of water is complex, involving a series of morphological, physiological and biochemical adjustments (Jiao et al., 2023; Lin et al., 2023; Marusig and Tombesi, 2020; Serra et al., 2014). Stomatal closure is one of the earliest responses and plays a key role in reducing water loss through transpiration. However, this mechanism also restricts the diffusion of CO_2 into the leaf, which reduces photosynthetic activity and growth (Jiao et al., 2023; Jones et al., 2022; Marusig and Tombesi, 2020; Zivcak et al., 2016). Intrinsic Water Use Efficiency (WUE_i), which is defined as the ratio of carbon dioxide assimilation to water transpired, varies widely among genotypes. It is also strongly influenced by their hydraulic behaviour, specifically whether they are isohydric or anisohydric (Schultz and Stoll, 2010; Van Leeuwen et al., 2019). Isohydric genotypes maintain relatively constant leaf water potential by regulating stomatal conductance. In contrast, anisohydric genotypes keep their stomata open even under water-limited conditions (Cogato et al., 2022; Jones et al., 2022).

Beyond these initial responses, grapevines activate molecular mechanisms to cope with prolonged drought. Osmotic adjustment, achieved by accumulating osmotically active compounds (osmolytes), is essential for maintaining cell turgor and sustaining metabolic processes under water-deficient conditions (Zivcak et al., 2016; Degu et al., 2019; Jones et al., 2022; Lin et al., 2023). Sugars are among the most abundant osmolytes. They help to maintain osmotic balance, protect cellular structures and provide energy for growth and recovery from stress (Ozturk et al., 2021; Zivcak et al., 2016). Drought stress triggers the production of reactive oxygen species (ROS), which can damage cell membranes, proteins and pigments if they are not effectively removed. Plants rely on antioxidant defence systems to counteract oxidative stress, and those with stronger antioxidant responses tend to be more tolerant of drought (Jiao et al., 2023; Lin et al., 2023).

While these intrinsic mechanisms are fundamental, agronomic strategies are equally important for mitigating the effects of drought. Grafting, for instance, is a vital viticultural practice. Originally an ancient horticultural technique, it was widely adopted in the 19th century to combat phylloxera, a devastating root pest. Today, grafting remains indispensable for conferring resistance to soil pathogens, improving nutrient uptake, and enhancing tolerance to abiotic stresses such as drought and salinity (Jiao et al., 2023; Marguerit et al., 2012). A grafted vine consists of two distinct genotypes: the scion, which determines the characteristics of the fruit, and the rootstock, which influences water and nutrient absorption, vigour, and resilience to stress. Grapevine rootstocks mitigate the negative effects of water scarcity on scions by adapting morphologically, physiologically and molecularly. They enhance scion performance by developing extensive, deep root systems that improve soil water exploration and increase root-to-shoot hydraulic conductance (Dattola et al., 2026; Marín et al., 2021). Experimental evidence shows that vigorous rootstocks, such as 1103 Paulsen or 140 Ruggeri, maintain higher stomatal conductance and photosynthetic rates during drought conditions by ensuring a consistent water supply to the leaves. This prevents a rapid drop in leaf water potential (Romero et al., 2025; Prinsi et al., 2021). Furthermore, rootstocks regulate scion responses through chemical signalling, primarily involving the synthesis of abscisic acid (ABA) in the roots. Tolerant genotypes often exhibit reduced ABA accumulation, delaying stomatal closure and sustaining carbon gain (Prinsi et al., 2021; Labarga et al., 2023). At a molecular level, rootstocks influence the expression of aquaporin genes (VvPIPs and VvTIPs) in the scion. These genes modulate membrane water permeability and facilitate faster recovery after re-watering (Labarga et al., 2023; Galaz et al., 2024). Studies involving leaf water potential measurements, whole-canopy gas exchange monitoring and untargeted metabolomics have shown that tolerant rootstocks such as M4 accumulate protective secondary metabolites, including stilbenes and folates, to counteract the oxidative stress caused by a lack of water (Lucini et al., 2020; Corso et al., 2015). Transcriptomic profiling confirms that rootstock genotype is critical in improving vineyard resilience to drought (Bianchi et al., 2018; Flor et al., 2025).

Since altering the scion genotype can have a significant impact on grape and wine quality, identifying new genotypes for use as rootstocks is becoming increasingly important. Therefore, selecting new rootstocks is a promising way to mitigate the effects of climate change on viticulture (Marguerit et al., 2012; Sucu et al., 2018). Despite these advances, a critical knowledge gap remains. For this reason, it is important to increase the number of rootstock genotypes and characterise their physiological and biochemical responses to water stress, in order to develop adaptive viticultural strategies.

The present study takes an integrated approach, combining photosynthesis analysis, sugar quantification and protein assays, in order to screen the response of non-commercial grapevine genotypes to controlled drought conditions. This includes physiological measurements, such as gas exchange and water use efficiency; biochemical assessments, such as sugar accumulation and stress-related proteins and oxidative stress-related parameters, such as total antioxidant power, total phenols, flavonoids and malondialdehyde (MDA). This work is characterised by its use of the state-of-the-art 'Microcosmo' system, a fully controlled, instrumented field simulator. This platform enables environmental variables to be manipulated precisely and plant performance to be monitored continuously. This overcomes the limitations of field trials, where environmental variability can obscure genotype-specific responses. The study aims to identify rootstocks that can show superior physiological plasticity under drought conditions. In combination with high-quality productive scions, this will promote the long-term sustainability of Mediterranean viticulture in the context of climate change.

2. Materials and methods

2.1. Grapevine genotypes

The experiment was carried out on six grapevine genotypes provided by the Department of Agricultural and Environmental Sciences, University of Milan. These genotypes belong to a *Vitis* spp. core-collection of 70 genotypes, which represent the whole genetic diversity of a germplasm collection of 232 rootstocks (Migliaro et al., 2019). These genotypes were selected for their contrasting responses to drought, as identified in preliminary screening trials on the core-collection (Table 1). The selected genotypes included two commercial rootstocks, namely 161.49-Couderc and Dog Ridge, displaying opposite putative drought responses.

Table 1
List of the commercial status and the genetic background of the six rootstock.

ID	Status	Sex_cod_OIV	Genetic background	Putative drought response
161.49-C	commercial	4	*Vitis riparia x Vitis Berlandieri*	Susceptible
Dog Ridge	commercial	4	*Vitis rupestris x Vitis candicans*	Tolerance
cc114	non-commercial	1	Unknown	Susceptible
cc125	non-commercial	4	*Vitis labrusca* Muncy	Tolerance
cc136	non-commercial	1	41 B Millardet et de Grasset x 31 Richter	Tolerance
cc177	non-commercial	1	Unknown	Susceptible

2.2. Experimental design

Four individuals were used for each genotype. Young cuttings were rooted at the University of Milan and then transferred to a controlled environment (Microcosmo; FOS S.p.A., Genoa, Italy and ENEA, Rome, Italy; https://pianogreen.com/microcosmo/) at the University of Siena. The substrate consisted of predominantly clay soil collected from a Chianti Classico farm (43.3496003943712, 11.501246996193618, Siena, Italy); The physical and chemical properties of the soil are listed in Table 2. A layer of universal potting soil was applied to the surface to facilitate planting. Inside the Microcosmo, a photoperiod of 16/8 with a red:blue light ratio of 3:1, a temperature of 25 °C (9 am - 7 pm) and 20 °C (remaining hours) and a humidity of 60% were maintained. Soil moisture was monitored using probes (TDSPSM02.015, Ageon, Cuneo, Italy) and kept at 60% by irrigation throughout the control period. After a 60-day acclimation period, drought stress was induced by withholding irrigation. The drought period was defined based on soil moisture content rather than duration, with three moisture ranges identified: Ctrl (control), pre-drought stress (PRE_DS, with moisture content between 40% and 50%), and DS (drought stress, with moisture content below 40%). After entering the DS phase, the stress period was divided into four time points: DS_1, DS_4, DS_6 and DS_8, which corresponded to the 1st, 4th, 6th and 8th day of the DS phase, respectively. At both the CTRL and DS_8 experimental phases, we harvested 12 fully expanded leaves per genotype (3 leaves collected from each of 4 individual plants). To ensure a representative composite sample and account for intra-plant variability, these 12 leaves were pooled and ground to a fine powder in liquid nitrogen. From this homogenized biological pool, aliquots were taken for downstream analyses.

Table 2
The physical and chemical characteristics of the soil used to grow the vines in the Microcosmo as provided by ISVEA (https://www.isvea.it, Poggibonsi, Siena, Italy).

Parameter	Value
Sand	42%
Silt	28%
Clay	30%
Coarse fragment	13%
Nitrogen	1.41 g/Kg
Organic matter	19.55 g/Kg
Limestone	7%
Assimilable phosphorous	18 mg/kg
Exchangeable Potassium	155 mg K/Kg
pH	8.1
Active limestone	1%
Cation exchange capacity	27.4 meq/100 *g*

2.3. Leaf gas exchange and chlorophyll fluorescence

Net carbon assimilation (A) and stomatal conductance (g_{sw}) parameters were recorded by a portable LI-6800 gas exchange analyzer (LI-COR Biosciences, Lincoln, NE, USA) equipped with an integrated chlorophyll fluorescence chamber at all time-points. During the measurements, the following conditions were set: 2 cm^2 chamber area, CO_2 at 400 ppm, 60% of relative humidity, block temperature at 25 °C, and photosynthetic active radiation (PAR) at 1600 µmol m^{-2} s^{-1}. Electron transport rate (ETR) and effective efficiency of PSII (ΦPSII) were measured on the same light-adapted leaves according to Gilbert et al. (2012). In addition, the maximum quantum yield of PSII (F_v/F_m) was measured in 4 dark-adapted leaves covered with aluminium foil for at least 30 min for each genotype. Intrinsic Water Use Efficiency (µmol CO_2 mmol H_2O^{-1}) was derived from the ratio of A to g_{sw}. Measurements were taken from five fully expanded leaves for each experimental group.

2.4. Protein extraction from grapevine leaves

Protein extraction was performed on CTRL and DS_8 leaf samples according to the protocol of Wu et al. (2014), as modified in Parri et al. (2024). Three samples of 0.3 g leaf powder ground in liquid nitrogen were prepared for each experimental group. Proteins were precipitated for 20 min at −20 °C with 1.8 mL cold 10% TCA/acetone solution containing 10 mM DTT. After centrifugation at 15,000 × g for 5 min at 4 °C, the pellets were washed three times with 80% cold acetone, air dried (~35–40 min), and resuspended in 0.8 mL SDS extraction buffer (1% SDS, 0.15 M Tris–HCl pH 8.8, 1 mM EDTA, 0.7 M sucrose, 1 mM DTT) and protease inhibitors. Samples were kept at room temperature for 1 h with gentle agitation. After centrifugation (15,000 × g, 10 min), the supernatants were collected in new tubes and an equal volume of Tris-buffered phenol (pH 7.8–8.0) was added, vortexed and centrifuged (15,000 × g, 10 min, 4 °C). The upper phenolic phase was collected, mixed with 4 vol of 0.1 M ammonium acetate in methanol, vortexed and stored at −20 °C for 2 h. Proteins were pelleted by centrifugation (15,000 × g, 10 min, 4 °C), washed with 0.1 M ammonium acetate in methanol and then with 80% acetone. After air drying the protein pellets, they were resuspended in 120 µL Laemmli buffer.

2.5. Electrophoresis and western blot

Proteins were separated on polyacrylamide gels run on 12% TGX Stain-Free FastCast gels (Bio-Rad, Hercules, CA). Unstained protein standard (Bio-Rad) was used as a molecular weight reference. Electrophoresis was performed at 200 V for 35 min in TGS buffer (25 mM Tris, 192 mM glycine, 0.1% SDS). Gels were imaged using ChemiDoc MP (Bio-Rad) with Stain-Free activation (UV exposure, 45 s) to visualize proteins without staining. Proteins were electrotransferred to nitrocellulose membranes using the Trans-Blot Turbo system (Bio-Rad) (1.3 A, 25 V, 5 min). Membranes were blocked with EveryBlot Blocking Buffer (Bio-Rad) for 5 min and washed twice in TBS 1X with 0.1% Tween-20. The primary antibodies (anti-HSP70, AS081371; Cu/Zn SOD, AS184243; PIP1, AS224816; and SUS1, AS152830; all from Agrisera AB, Vännäs, Sweden) were diluted in blocking buffer and incubated for one hour with gentle rocking. After washing, the membranes were incubated with goat anti-rabbit IgG StarBright Blue 700 secondary antibody (Bio-Rad, diluted 1:2500) for 1 h. Protein transfer efficiency was confirmed by Stain-Free blot imaging. A quantitative analysis was performed using the total protein normalisation workflow in Image Lab (Bio-Rad). First, the lanes were automatically detected, and manual adjustments were made where necessary to ensure precise definition of the boundaries. The total protein signal for each lane was then calculated by integrating the intensity of all proteins visualised in the Stain-Free image. The normalisation factor for each sample was derived by dividing the total protein signal for each lane by the signal for the reference lane (typically the control group) on the same gel. The intensity of each target

immunoreactive protein band was then divided by its corresponding lane-specific normalisation factor. This method was chosen over the use of traditional housekeeping proteins in order to overcome issues related to protein saturation and biological variability. This provides a more accurate representation of relative protein content across all samples.

The graphs in the results section show the variation of the stressed group compared to its respective control group. This is calculated as follows: $(DS - CTRL) \ / \ CTRL\ 100$.

2.6. Sugar content analysis

For soluble sugar extraction, 0.2 g of leaf powder was dried at 70 °C for 24 h to determine dry weight (DW) according to Parri et al. (2024). 1 mL of distilled water was added to each sample. The tissue was then homogenised using a Mixer Mill MM 400 (Retsch GmbH, Haan, Germany) for 2 min at 50 Hz, after which it was incubated at 60 °C for 10 min and treated with ultrasound for a further 15 min. After centrifugation at 16,000× *g* for 5 min, the supernatant was collected and the pellet was subjected to a second extraction. The combined supernatants were filtered (0.45 μm). High performance liquid chromatography was performed by ISVEA (https://www.isvea.it/, Poggibonsi, Siena, Italy) according to OIV-MA-AS311–03 protocol (https://www.oiv.it). Results are expressed in mg/g DW as the mean ± standard deviation of three replicates. The graphs in the results section show the variation of the stressed group compared to its respective control group. This is calculated as follows: $(DS - CTRL) \ / \ CTRL\ 100$.

2.7. Determination of antioxidant capacity, total polyphenols and flavonoids

To evaluate the antioxidant capacity, as well as the total polyphenol and flavonoid content, the leaf powder was extracted using a 1:6 (w:v) solution of 70% acetone. All spectrophotometric measurements were performed in triplicate. Total antioxidant capacity was determined using the ferric reducing antioxidant power (FRAP) method (Benzie and Strain, 1996). For each measurement, 204 μL of 300 mM acetate buffer solution (pH 3.6), 20 μL of 10 mM TPTZ (2,4,6-tripyridyl-s-triazine) solution, 20 μL of 20 mM ferric chloride solution, and 2 μL of the extract (70% acetone for the blank) were mixed. The reaction mixture was then incubated at 37 °C for 1 h and the absorbance was recorded at 593 nm using a Multiscan SkyHigh Plate Reader (Thermo Fisher Scientific, Waltham, MA, USA). The results were calculated against a ferrous sulphate calibration curve and expressed as μmol Fe^{2+} equivalents per g of fresh weight.

The total polyphenol content was determined using the Folin–Ciocalteu colorimetric method (Singleton and Rossi, 1965). The reaction mixture was prepared by adding 10 μL of the extract (70% acetone for the blank), 230 μL of distilled water, 12.5 μL of Folin–Ciocalteu reagent and 37.5 μL of a saturated sodium carbonate solution. The mixture was then incubated at 37 °C for 30 min and the absorbance was measured at 795 nm using a Multiscan SkyHigh Plate Reader (Thermo Fisher Scientific, Waltham, MA, USA). Total polyphenol concentration was calculated from a gallic acid standard curve and expressed as milligrams of gallic acid equivalents (GAE) per g of fresh weight.

Total flavonoid content was determined using the aluminium chloride colorimetric method (Smirnova and Pervykh, 1998). The reaction mixture was prepared by adding 12.5 μL of the extract (70% acetone for the blank), 75 μL of 95% ethanol, 5 μL of 10% aluminium chloride, 5 μL of 9.8% potassium acetate and 152 μL of distilled water. The mixture was then incubated at room temperature for 1 h and the absorbance was measured at 415 nm using a Multiscan SkyHigh Plate Reader (Thermo Fisher Scientific, Waltham, MA, USA). Total flavonoid concentration was calculated using a quercetin standard curve and expressed as milligrams of quercetin equivalents (QE) per g of fresh weight.

2.8. Malondialdehyde content

The malondialdehyde (MDA) content was used to quantify the level of lipid peroxidation in the leaves. 0.1 g of leaf powder was weighed into a tube containing 1.5 ml of 0.1% trichloroacetic acid (TCA). The samples were then centrifuged at 10,000 g for 10 min at 4 °C. For the positive control, 0.25 mL of the supernatant (0.1% TCA for blank) was mixed with 1 mL of 20% TCA containing 0.5% (w/v) thiobarbituric acid. For the negative control, the same supernatant (0.1% TCA for blank) was mixed with 1 mL of 20% TCA alone. The samples were incubated for 30 min at 95 °C, after which the extracts were immediately cooled on ice and centrifuged at 10,000 g for 10 min at 4 °C. The absorbance of the positive and negative control samples was measured at 600, 532 and 400 nm using an EnSpire microplate reader (PerkinElmer, Waltham, MA, USA). MDA equivalents were calculated according to Hodges et al. (1999) and normalised to fresh weight. The assay was conducted in three technical replicates.

2.9. Statistical analysis

The normality of the distribution of the data on physiological measurements and sugar quantification was assessed using the Shapiro–Wilk test, and homoscedasticity was evaluated using Levene's test. A 2-way ANOVA was performed to assess the significant effects of genotype (G), irrigation treatment (S) and their interactions (G x S). Where ANOVA yielded a significant result ($p < 0.05$), a Tukey's HSD *post hoc* test was performed to identify which groups differed significantly from each other. All graphs were generated using the ggplot2 package in RStudio.

3. Results

The first part of the results section provides an overview of the variability observed in physiological parameters under drought stress. Table 3 reports the statistical significance of the main factors ("Genotype" and "Treatment") and their interaction as assessed by ANOVA. All parameters were significantly affected by "Genotype" and "Genotype x Treatment". Indeed, the factor "Treatment" affected all parameters except F_v/F_m. Cc177 showed the lowest values in all physiological parameters. Regarding the treatments, stomatal conductance decreased linearly with an increase in stress, as did net carbon assimilation. The highest water use efficiency values were reached at DS_4. Photosynthetic parameters (ΦPSII and ETR) remained steady until DS_4, after which they decreased abruptly.

Overall, all rootstock genotypes exhibited a decline in stomatal conductance from the control phase through to the stress phases (PRE_DS to DS_8), as shown in Fig. 1A. This indicates that a water deficit reduces stomatal conductance in all rootstocks. Dog Ridge is the only genotype that exhibited an early and rapid decrease at the PRE_DS/DS_1 stage. Other genotypes (e.g. 161.49-C, cc125, cc136) exhibited a linear decrease from the DS_1 stage, whereas cc114 and cc177 displayed a more gradual decline throughout the stress period. Furthermore, cc114 at the DS_6 stage exhibited partial indications of stomata opening.

Significant differences in net carbon assimilation were observed among the various genotypes (Fig. 1B). Some genotypes (161.49-C, Dog Ridge, cc125 and cc136) exhibited increased A values due to water scarcity during the initial stress phases. cc125 and cc136, in particular, showed an increase in this value up to DS_4; after this point, it decreased in subsequent stages. Conversely, 161.49-C and Dog Ridge exhibited this increase at DS_1, after which it fell rapidly. Genotypes such as cc114 and cc177 were more sensitive, showing an early decline in net carbon assimilation from DS_1 onwards.

As can be seen in Fig. 1C, all genotypes showed a decline in WUE_i at DS_8, with cc177 experiencing the most significant decrease. During the initial phase of the DS, differences emerged: Dog Ridge and cc125 showed an increase at DS_1, DS_4 and DS_6, respectively, while WUE_i remained stable in all other genotypes.

Table 3
Summary of 2-way ANOVA and Tukey's HSD test for the effects of "Genotype" (G), "Treatment" (S), and their interaction (G × S) on the following parameters: stomatal conductance (g_{sw}), net CO_2 assimilation (A), intrinsic water use efficiency (WUE_i), the maximum quantum efficiency of PSII (F_v/F_m), quantum yield of photosystem II (ΦPSII) and electron transport rate (ETR). Each value represents the mean of measurements taken on 5 fully expanded leaves ± standard deviation. Asterisks indicate levels of statistical significance according to ANOVA test (* p-value < 0.05, *** p-value< 0.001). Different letters denote significant differences according to Tukey post-hoc test.

	g_{sw}	A	WUE_i	F_v/F_m	ΦPSII	ETR
Genotype (G)						
161.49-C	0.08 ± 0.08 ab	4.72 ± 4.37 ab	54.25 ± 64.17 bc	0.75 ± 0.02 b	0.03 ± 0.02 b	23.82 ± 14.53 b
Dog Ridge	0.09 ± 0.12 a	4.23 ± 3.43 b	77.78 ± 65.41 ab	0.77 ± 0.01 a	0.03 ± 0.01 ab	24.66 ± 10.86 ab
cc114	0.06 ± 0.03 bcd	4.21 ± 2.88 b	72.96 ± 46.37 bc	0.76 ± 0.02 ab	0.03 ± 0.01 ab	25.58 ± 11.22 ab
cc125	0.05 ± 0.04 cd	4.89 ± 3.14 ab	119.67 ± 141.34 a	0.75 ± 0.02 b	0.03 ± 0.02 a	28.84 ± 13.34 a
cc136	0.07 ± 0.05 abc	5.53 ± 3.74 a	73.67 ± 57.23 bc	0.76 ± 0.02 ab	0.03 ± 0.02 ab	28.01 ± 13.86 ab
cc177	0.04 ± 0.03 d	2.97 ± 2.20 c	32.44 ± 137.37 c	0.76 ± 0.02 ab	0.02 ± 0.01 c	17.62 ± 7.05 c
p-value	< 0.001 ***	< 0.001 ***	< 0.001 ***	0.0113 *	< 0.001 ***	< 0.001 ***
Treatment (S)						
CTRL	0.11 ± 0.10 a	5.27 ± 1.68 b	68.85 ± 38.71 b	0.76 ± 0.02	0.04 ± 0.01 a	30.78 ± 9.58 a
PRE_DS	0.10 ± 0.05 ab	6.79 ± 1.32 a	81.65 ± 37.84 b	0.76 ± 0.02	0.04 ± 0.01 a	31.97 ± 9.10 a
DS_1	0.09 ± 0.05 b	6.96 ± 3.32 a	88.07 ± 36.12 b	0.76 ± 0.01	0.04 ± 0.01 a	30.84 ± 9.63 a
DS_4	0.04 ± 0.02 c	5.43 ± 3.46 b	148.56 ± 101.14 a	0.76 ± 0.02	0.03 ± 0.01 a	28.68 ± 9.54 a
DS_6	0.03 ± 0.03 cd	2.23 ± 1.64 c	98.32 ± 60.01 b	0.75 ± 0.02	0.02 ± 0.01 b	19.83 ± 7.71 b
DS_8	0.01 ± 0.01 d	−0.15 ± 0.38 d	−54.67 ± 122.55 c	0.75 ± 0.02	0.01 ± 0.00 c	6.43 ± 4.20 c
p-value	< 0.001 ***	< 0.001 ***	< 0.001 ***	0.1149	< 0.001 ***	< 0.001 ***
G x S						
p-value	< 0.001 ***	< 0.001 ***	< 0.001 ***	0.0132 *	< 0.001 ***	< 0.001 ***

No substantial differences in maximum PSII efficiency values (Fig. 1D) were observed between the different genotypes under the various sampling conditions. As shown in Fig. 1e, there were no statistically significant differences, with values remaining consistently at around 0.75, which suggests that PSII efficiency was adequately maintained.

With regard to the values of PSII efficiency (Fig. 1E) and the electronic transport rate (Fig. 1F), 161.49-C exhibited an increase in these parameters up to DS_1, after which they decreased rapidly. The cc125 and cc136 genotypes exhibited stable values up to DS_4, after which they decreased in subsequent stages. The cc114 genotype only decreased ETR and ΦPSII at the PRE_DS stage, followed by a plateau until DS_8; thereafter, it decreased. The Dog Ridge and cc177 genotypes showed a slow and steady decrease in ETR and ΦPSII.

Fig. 2A shows blots relative to superoxide dismutase (SOD), sucrose synthase (SuSy), the plasma membrane intrinsic protein (PIP1) subfamily of aquaporins, and the heat shock protein (HSP70). Analysis of superoxide dismutase levels (Fig. 2B) revealed significant heterogeneity in the oxidative stress response among the examined rootstock genotypes under water deficit conditions. While most genotypes showed an increase in SOD protein content, indicating an enhanced antioxidant defence, the extent of this response varied considerably. The most pronounced increase was observed in cc125, with a striking +272.1% increase relative to the control. Significant increases were also observed in Dog Ridge (+146.9%), cc177 (+120.4%), cc114 (+83.4%) and 161.49-C (+47.2%), indicating that these genotypes had activated different but notable antioxidant pathways. In contrast, cc136 was the only genotype to undergo a significant reduction in SOD content (−68.6%), suggesting a weaker or differently regulated oxidative stress response mechanism. Overall, these findings emphasise the substantial variation in antioxidant capacity among different genotypes.

Analysis of sucrose synthase levels (Fig. 2C) revealed an upward trend in all tested grapevine rootstock genotypes when exposed to drought stress. This uniform increase suggests that SuSy-mediated carbohydrate metabolism is a broadly conserved response to water deficit. Genotype cc125 displayed the strongest reaction again, with SuSy accumulation rising by 175% compared to the control. This indicates a particularly robust adjustment of sucrose metabolism, while cc136 followed with an increase of 126.6%. Significant, albeit more moderate, increases were also observed in 161.49-C (63.6%), Dog Ridge (43.7%) and cc114 (32.1%). In contrast, cc177 exhibited a modest increase of only 12%.

Quantification of aquaporin proteins in leaf tissues (Fig. 2D) revealed notable genotype-specific responses to drought stress. The highest levels of PIP1 upregulation were measured in cc136 and cc114 (+72.8% and +71%, respectively). Significant, albeit lower, increases were also observed in 161.49-C (+38.7%) and cc125 (+24.2%). By contrast, Dog Ridge exhibited only a slight increase of +8.1%. Interestingly, cc177 was the only genotype to experience a significant decrease in PIP1 content (−26.2%).

As shown in Fig. 2E, drought stress caused significant genotype-dependent changes in HSP70 protein accumulation in leaf tissues. Genotype cc125 displayed the most substantial increase, with HSP70 levels rising to 116.5% relative to the well-watered control. Cc114 also exhibited a significant increase of 93.8%. By contrast, 161.49-C and Dog Ridge showed modest increases of 13.6% and 6.7% respectively. Meanwhile, cc136 and cc177 experienced significant decreases of −30.6% and −26.9% respectively.

Two-way ANOVA revealed that genotype, treatment and their interaction significantly influenced both glucose and fructose content (p value < 0.001). The analysis of leaf glucose levels (Fig. 3A) revealed a genotype-dependent response to drought stress, largely mirroring the trends observed for fructose (Fig. 3B). In most genotypes, water deficit induced a significant accumulation of these sugars, consistent with the role of hexoses in osmotic adjustment. The genotypes cc114 exhibited the most robust response, achieving the highest variation in glucose and fructose concentrations under drought stress (both + 64.3%), reaching 47 mg/g DW (Table 4). Significant sugars accumulation was also observed in cc177, 161.49-C, and cc125, which showed the highest glucose and fructose content under drought stress. Conversely, the cc136 genotype showed no significant difference between the control and stressed samples, maintaining steady glucose and fructose levels in both conditions. Contrary to the other genotypes, Dog Ridge exhibited a substantial and significant decrease in glucose and fructose content, dropping from approximately 48 mg/g DW of glucose in control to 32 mg/g DW under stress and from 46 mg/g DW of fructose to 21 mg/g DW.

The total antioxidant content of grapevine genotypes (Fig. 4A) varied significantly and showed a genotype-specific response to water deficit. Among well-watered plants, cc136 had the highest antioxidant content, followed by cc114; cc125 had the lowest level. Water deficit increased antioxidant accumulation in several genotypes, although the magnitude of the response differed substantially. The greatest relative increase was observed in cc125 (+121.7%), followed by Dog Ridge (+40.9%) and cc114 (+14%). A slight increase was detected in cc177 (+3.4%), while

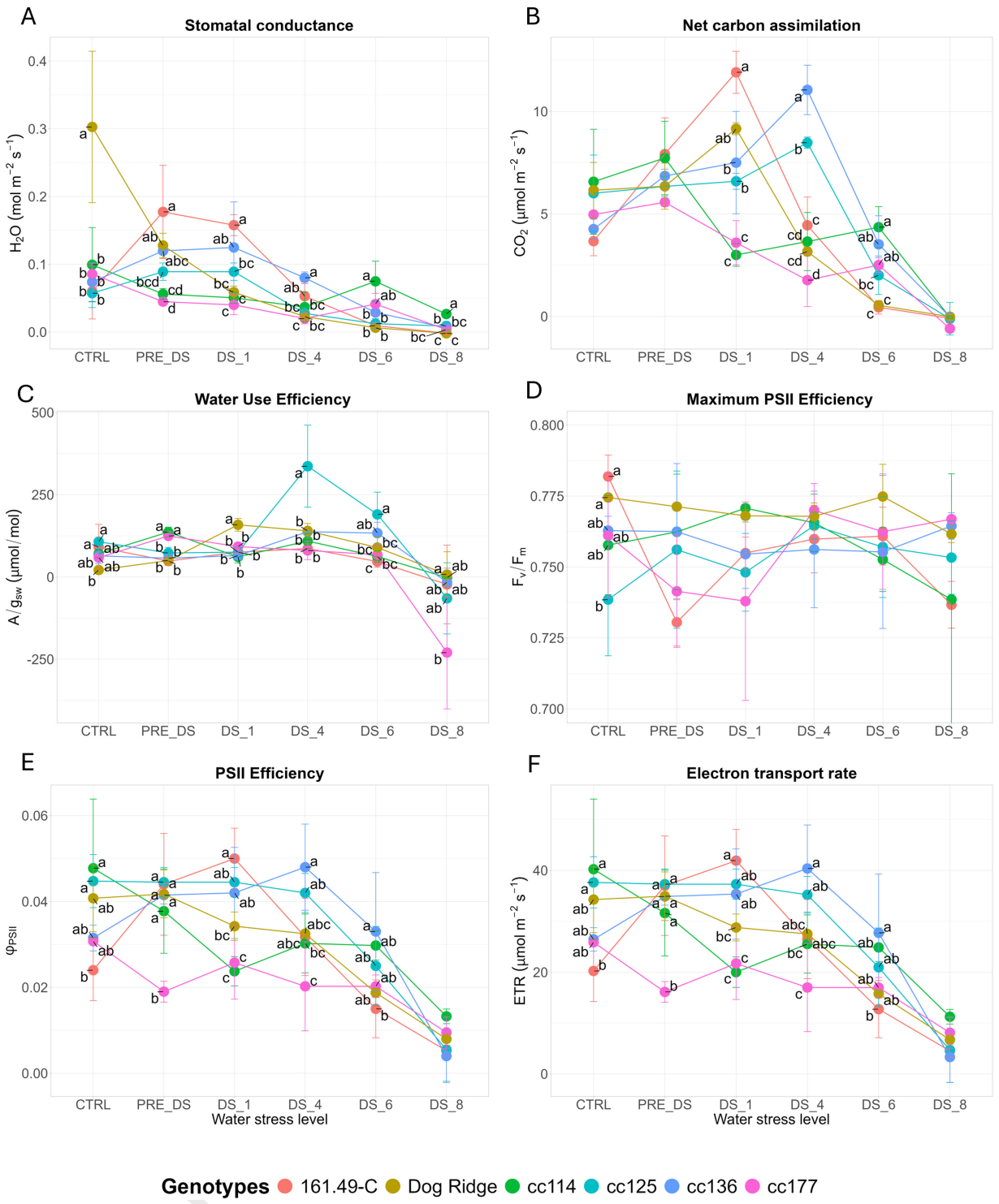

Fig. 1. Physiological responses of six grapevine rootstock genotypes during progressive water stress, from control (CTRL) to pre-stress phase (PRE_DS) to DS_8 stage. (A) Stomatal conductance (g_{sw}); (B) Net CO_2 assimilation (A); (C) Intrinsic water use efficiency (WUE_i); (D) Maximum PSII efficiency (F_v/F_m); (E) PSII quantum efficiency (ΦPSII); (F) Electron transport rate (ETR). Data are mean ± SD; different letters indicate significant differences according to Tuckey post-hoc test.

antioxidant content decreased in 161–49.C (−8%) and cc136 (−17.3%) under stressful conditions. Despite the significant relative increase observed in cc125, its absolute antioxidant content under stress conditions was lower than that measured in cc114 and cc136. Conversely, cc114 exhibited a high basal antioxidant content which increased further under water deficit, resulting in the highest values under stress.

Total phenolic content (Fig. 4B) varied significantly between grapevine genotypes and demonstrated a distinct genotype-dependent response to water deficit. Under well-watered conditions, cc114 exhibited the highest phenolic levels, while cc125 displayed the lowest content. Water deficiency significantly increased phenolic accumulation in some genotypes, notably cc125 (+152.6%) and cc136 (+110%). However, despite the significant relative increase in cc125, its absolute phenolic content remained lower than that of cc114 and cc136, the two lines that maintained the highest levels overall. Cc136 exhibited high basal levels and strong inducibility, while cc114 demonstrated stable

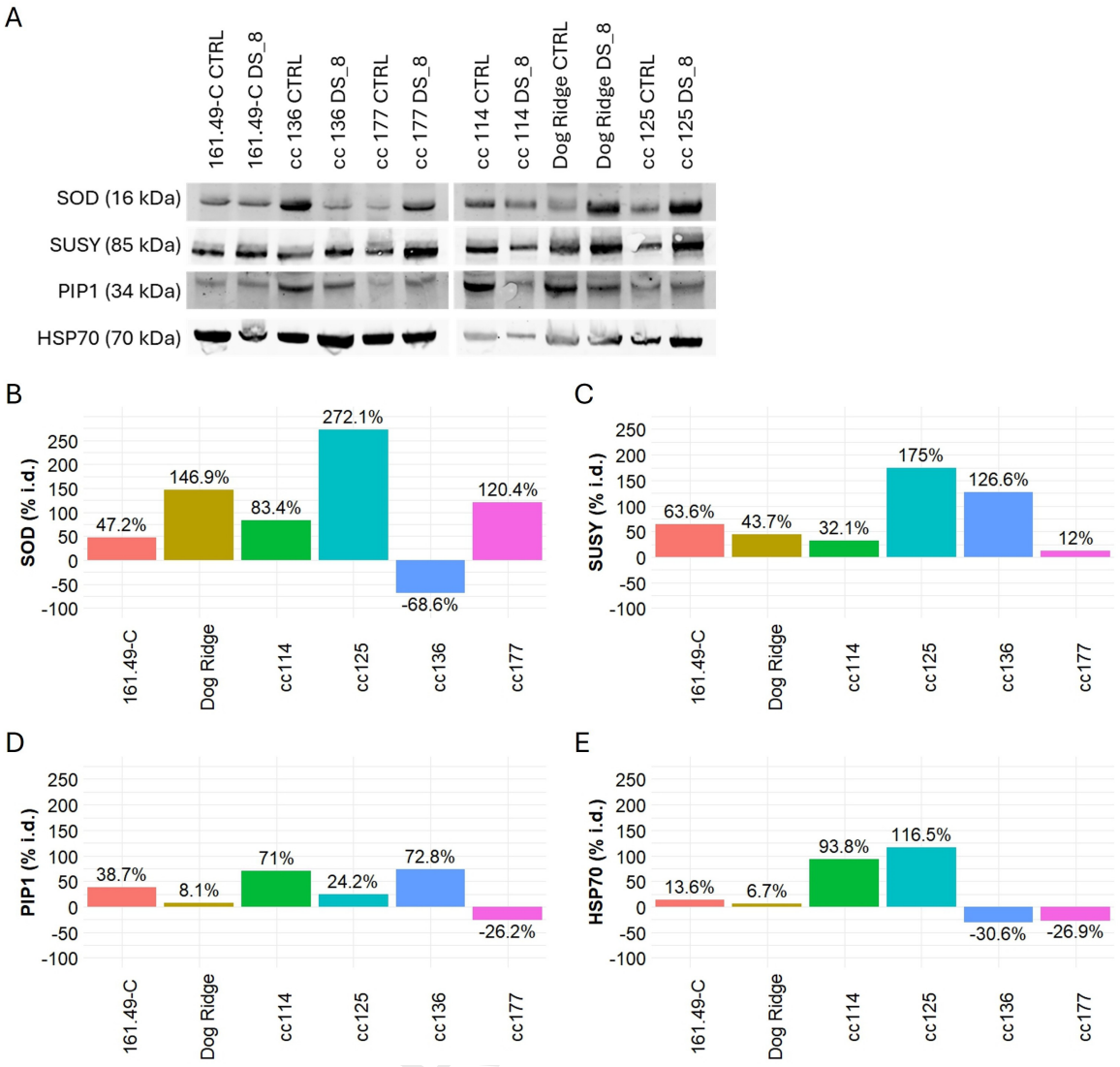

Fig. 2. Relative changes in protein content in the leaves of six grapevine rootstock genotypes (161.49-C, Dog Ridge, cc114, cc125, cc136, and cc177) under drought stress (DS). Values are expressed as a percentage of the water-stressed sample relative to the well-watered control (CTRL). The original blots are at the top (A), and the graph below shows the relative protein changes after normalisation to the protein content in each lane. (B) Changes in superoxide dismutase (SOD) protein content. (C) Relative variation of sucrose synthase (SuSy) protein content. (D) Relative variation of aquaporin (PIP1) protein content. (E) Changes in Heat Shock Proteins (HSP70) content.

and consistently high phenolic content.

The total flavonoid content (Fig. 4C) varied among the grapevine genotypes, showing a clear genotype-specific response to water deficit. Under well-watered conditions, cc114 and cc136 exhibited the highest flavonoid levels, whereas cc125 and Dog Ridge exhibited lower levels. Under stress conditions, cc114 showed a substantial increase of 52%, reaching the highest overall values. By contrast, the flavonoid content decreased markedly in 161–49.C and Dog Ridge, and remained essentially unchanged in cc125, cc136 and cc177.

The MDA content (Fig. 5) increased consistently in response to water deficit in all genotypes, indicating enhanced lipid peroxidation under stress conditions, except for 161.49-C. Among well-watered plants, cc177 and cc114 exhibited the lowest MDA levels, while higher baseline values were observed in all other genotypes. Under water deficit Dog Ridge and cc136 showed a particularly strong responses. Although cc114 and cc177 also showed increases, their absolute values remained lower than those of the genotypes that were more severely affected. The Cc125 value increased by 48%, reaching the highest recorded level under drought stress.

4. Discussion

Water deficit triggers a highly coordinated cascade of physiological, biochemical, and molecular responses in grapevines. Stomatal closure represents the first line of defence, limiting water loss while restricting CO_2 assimilation and driving downstream metabolic rebalancing (Bianchi et al., 2023). This hydraulic adjustment promotes ROS accumulation directly linking oxidative stress responses (Ismail et al., 2025; Nazir et al., 2022). Concurrently, molecular chaperones including HSP70 preserve protein and membrane integrity (Corso et al., 2015; Liu et al., 2022). Osmotic adjustment through compatible solute accumulation further stabilises cellular function, with SUSY activity connecting carbon partitioning to root hydraulic maintenance via aquaporins (Krishankumar et al., 2025; Prinsi et al., 2018). These mechanisms form an integrated network in which physiological plasticity is sustained by coordinated biochemical and molecular reprogramming. Identifying genotype-specific regulatory strategies represents a critical step towards the selection of more resilient rootstocks suited to future climatic conditions.

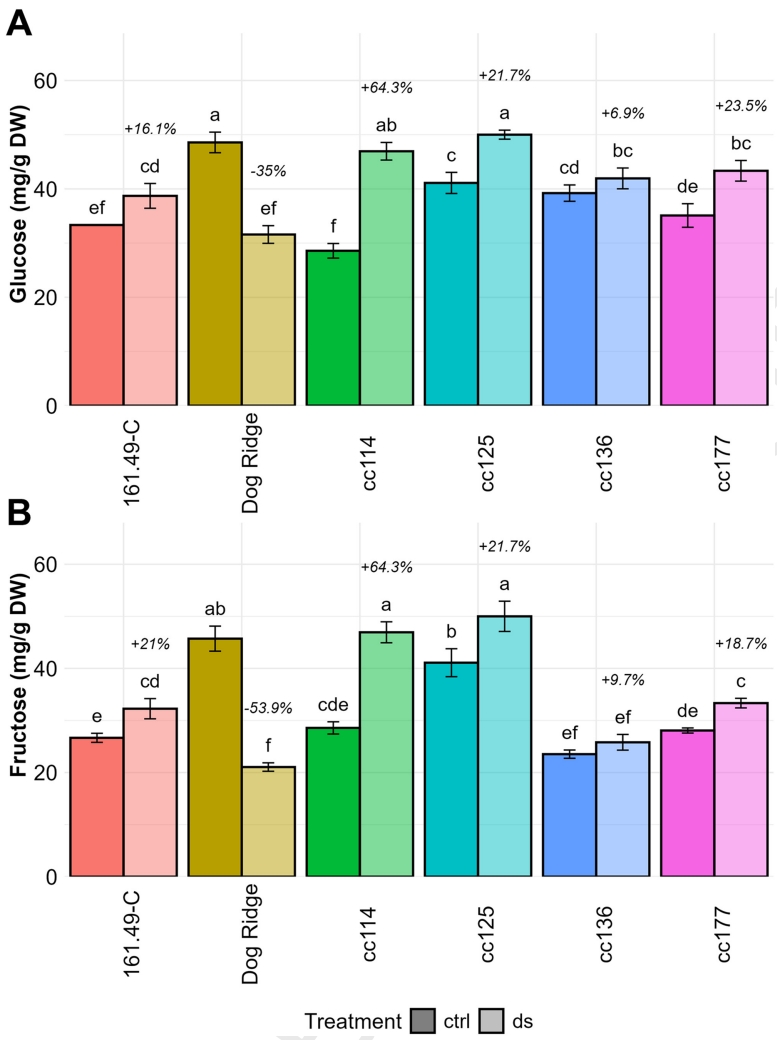

Fig. 3. Glucose (A) and fructose (B) content in the leaves of six grapevine rootstock genotypes (161.49-C, Dog Ridge, cc114, cc125, cc136, and cc177) under control (ctrl) and drought stress (ds) conditions. Each value represents the mean of three technical replicates from a biological pool ± standard deviation. Percentages above "ds" bars indicate the relative change compared to the respective control. Different letters denote significant differences according to Tukey post-hoc test ($p < 0.05$).

Water transport and carbon assimilation under drought stress

The findings concerning the physiological responses of six grapevine rootstocks confirm that the genotype of the rootstock significantly influences the plant's strategy for coping with a progressive water deficit (Bianchi et al., 2020), as can be seen in Table 3. From a physiological perspective, three different macro-patterns can be observed: *i)* 161.49-C, cc125 and cc136 showed an increase in gas exchange parameters and photosynthetic performance during the initial stage of drought stress. These genotypes had an anisohydric behaviour that suggests a capacity for drought acclimation comparable to that observed in the M4 rootstock, which is considered a drought tolerant-genotype (Merli et al., 2016; Meggio et al., 2014). An increase in stomatal conductance has already been observed in grapevines under moderate drought stress (Gutiérrez-Gamboa et al., 2019) these genotypes are probably able to maintain photosynthetic activity by preserving root integrity and functionality more effectively (Prinsi et al., 2021). In addition, the WUEi for the cc125 up to the DS_6 suggests an effective equilibrium between the acquisition of carbon and the loss of water, which is a characteristic that is often sought when selecting rootstocks for semi-arid regions (Bianchi and Brancadoro, 2021); *ii)* cc114 and cc177 exhibited a slight and consistent decrease in all parameters throughout the entire stress period with a distinct recovery pattern at DS_6. Stomatal closure during the stress indicates a strategy for avoiding drought (Meggio et al., 2014). This behaviour is typical of genotypes that prioritise maintaining steady leaf water potential by swiftly closing their stomata, even at the cost of early reductions in carbon assimilation (Bianchi et al., 2020), as it was found in susceptible commercial stocks, such as SO4, where stomatal limitations quickly lead to a decrease in photosynthesis (Galbignani et al., 2016; Koundouras et al., 2008); *iii)* Dog Ridge exhibits an intermediate pattern: although the total conductance decreased initially, the steady photosynthetic efficiency resulted in the subsequent maintenance of net carbon assimilation at DS_1. These photosynthetic oscillations among the genotypes could not be explained by PSII impairment, since maximum PSII efficiency remained stable at around 0.75. This suggests that the structural integrity of the photosystem II reaction centres has largely been maintained (Jiao et al., 2023) and that, while its operating capacity can be impaired by non-stomatal factors or photoinhibition, the machinery remains intact (Galbignani et al., 2016; Meggio et al., 2014).

Gas exchange in grapevines was demonstrated to be regulated not only by ABA, but also by hydraulic conductivity from root to leaf, which is widely allowed by PIP1 (Khadka et al., 2019; Marusig and Tombesi, 2020). Aquaporins PIP1 are essential membrane proteins that regulate the hydraulic conductivity of cells by facilitating the movement of water and small solutes across plasma and vacuolar membranes (Koc et al., 2023; Maurel et al., 2015). Under drought conditions, modulating aquaporin expression is crucial for maintaining cellular turgor and managing

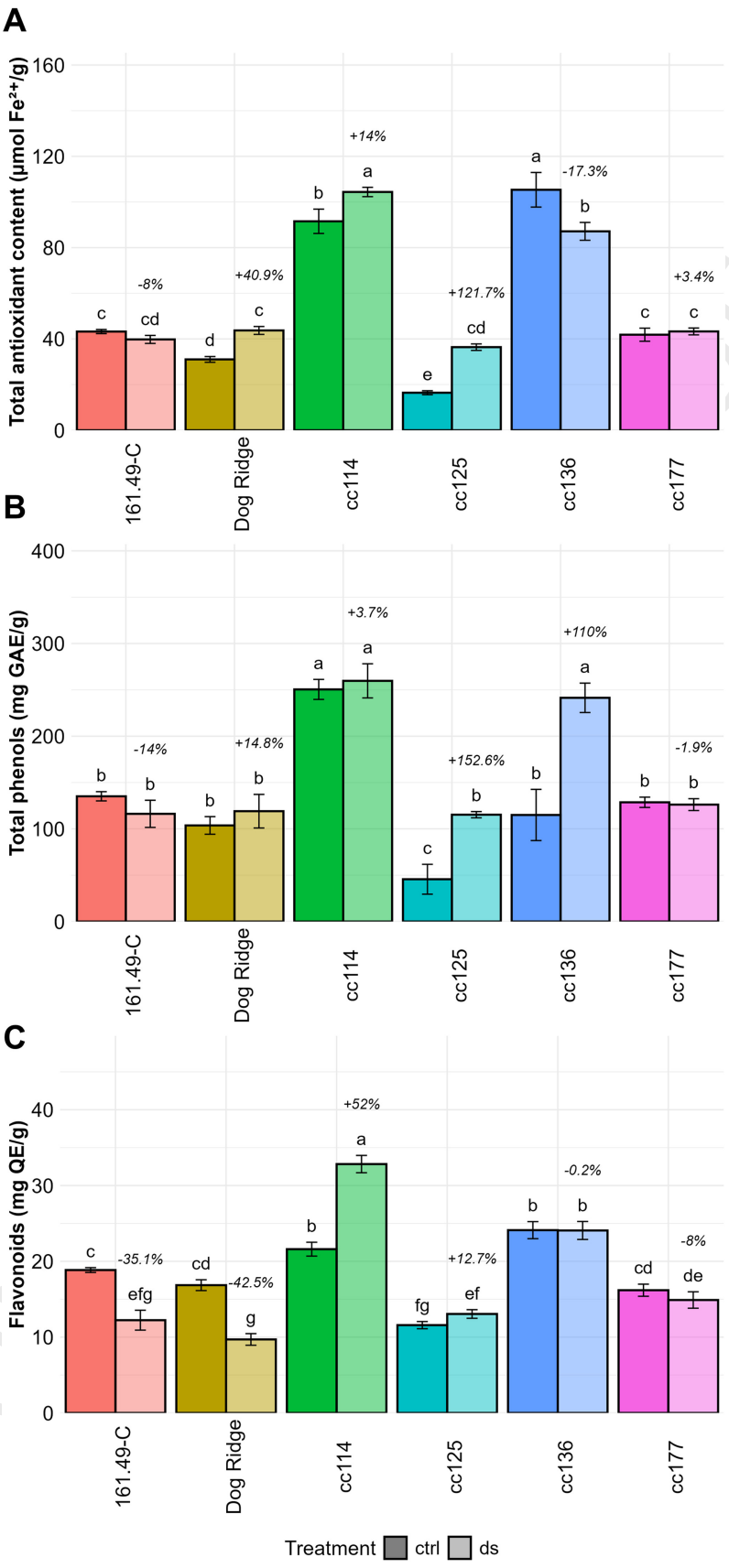

(*caption on next page*).

Fig. 4. Total antioxidant power (A), total phenols (B) and flavonoids (C) content in the leaves of six grapevine rootstock genotypes (161.49-C, Dog Ridge, cc114, cc125, cc136, and cc177) under control (ctrl) and drought stress (ds) conditions. Each value represents the mean of three technical replicates from a biological pool ± standard deviation. Percentages above "ds" bars indicate the relative change compared to the respective control. Different letters denote significant differences according to Tukey post-hoc test ($p < 0.05$).

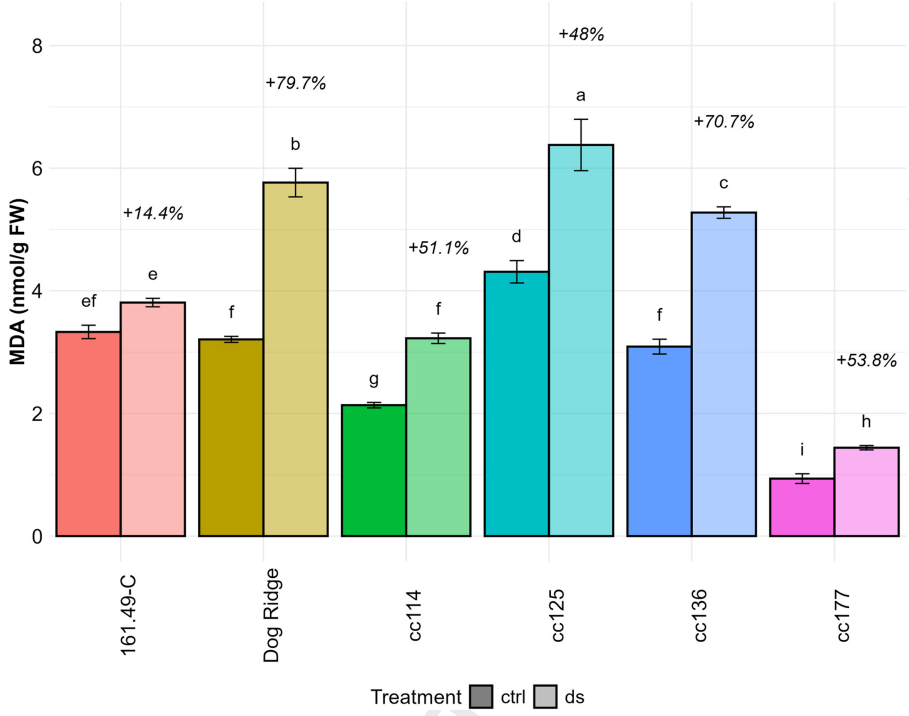

Fig. 5. MDA content in the leaves of six grapevine rootstock genotypes (161.49-C, Dog Ridge, cc114, cc125, cc136, and cc177) under control (ctrl) and drought stress (ds) conditions. Each value represents the mean of three technical replicates from a biological pool ± standard deviation. Percentages above "ds" bars indicate the relative change compared to the respective control. Different letters denote significant differences according to Tukey post-hoc test ($p < 0.05$).

internal water distribution in grapevines (Pou et al., 2013; Sabir et al., 2021). The significant upregulation observed in genotype cc136, coupled with the maintenance of the basal gas exchange rate, suggests anisohydric behaviour. This means that the plant maintains high water channel activity, enabling water to flow into its tissues despite decreasing soil water potential (Galaz et al., 2024; Labarga et al., 2023). Conversely, the downregulation of aquaporins in cc177 (−26.2%), confirms the water conservation strategy suggested by its low stomatal conductance (Bianchi et al., 2023; Vandeleur et al., 2009). Ultimately, the induction of PIP1 in genotypes such as 161.49-C, cc114, cc125 and cc136 demonstrates a high degree of biochemical plasticity. This enables these rootstocks to thrive in arid environments by maintaining efficient water transport systems (Savic et al., 2004; Yıldırım et al., 2018). Another important mechanism for managing water in grapevines is regulating soluble sugars. These act as an osmotic driving force, keeping water in leaf cells by reducing their inner water potential (Singh et al., 2015). Sucrose synthase is a key enzyme in grapevine sugar metabolism, enabling the reversible conversion of sucrose into fructose and UDP-glucose (Li et al., 2024). Consistent upregulation of SuSy across all rootstock genotypes under drought stress indicates a vital physiological adaptation for managing carbon resource allocation and sugar signalling (Ye et al., 2023; Li et al., 2024). The substantial increases in glucose and fructose observed in all genotypes confirmed the accumulation of the necessary hexoses for osmoprotection. However, in Dog Ridge and cc136, glucose and fructose could be allocated to other structural functions (Amor et al., 1995).

Finally, an imbalance in water management led to a deficiency of water in the leaves, which caused protein denaturation and aggregation (Waters et al., 1996). The HSPs protein family consists of molecular chaperones that stabilize proteins and membranes and refold proteins during environmental challenges such as drought, heat, and cold (Liu et al., 2022; Venios et al., 2020). In this study, HSP70 content varied significantly among grapevine rootstocks, highlighting distinct genotypic defense strategies. Cc125 and cc114 exhibited substantial induction of this protein (+116.5% and +93.8%, respectively), indicating the active protection of cellular structures typically associated with enhanced capacity to withstand stressful conditions tolerance (Ju et al., 2021; Savic et al., 2004). In contrast, genotypes cc136 and cc177 showed significant reductions in HSP70 content (−30.6% and −26.9%, respectively), suggesting impaired or overloaded protein synthesis systems. This is a common feature of sensitive varieties, where stress results in metabolic inhibition (Azri et al., 2020; Guo et al., 2025). These findings demonstrate that different grapevine rootstocks employ distinct biochemical mechanisms to cope with water scarcity: some successfully upregulate protective chaperones, while others experience a collapse in their stress response machinery (Azri et al., 2020; Liu et al., 2022).

Oxidative stress responses and cellular protection mechanisms

Restricted gas exchange typically results in an imbalance between light absorption and CO_2 fixation, which drives the accumulation of reactive oxygen species. The accumulation of ROS leads to oxidative stress, causing damage to vital cellular components, including lipid membranes, via lipid peroxidation (Haider et al., 2017; Lin et al., 2023). This can be measured by the content of malondialdehyde. Although MDA is a standard indicator of lipid peroxidation and oxidative damage, it is important to note that lipid peroxidation functions as both a damage process and a component of stress signaling (Morales and Munné-Bosch, 2019). The only genotype that did not exhibit a significant difference was 161.49-C. Its low level of membrane damage, as indicated by MDA

content closely resembling that of the control, appears to result from the strict regulation of ROS synthesis rather than from scavenging mechanisms, given the absence of substantial increases in antioxidant defenses. This aligns with physiological observations: maintaining basal gas exchange rates prevents ROS formation within thylakoid membranes, a process typical of light stress. Increased MDA levels were observed in all genotypes under drought stress, confirming that a water deficit induces oxidative stress at the membrane level. However, specific antioxidant and defensive response patterns could be identified. Nevertheless, these failed to significantly reduce lipid peroxidation in leaf membranes. The highest accumulation of MDA compared to the control group occurred in Dog Ridge and cc136, suggesting that these genotypes experienced significant lipid peroxidation despite showing two different biochemical response strategies. While cc136 did not demonstrate increased antioxidant capacity or enzymatic antioxidant defences, Dog Ridge exhibited significant SOD upregulation, which was probably insufficient to counteract ROS production alone. SOD is considered the first line of defence in the plant's antioxidant system, as it converts superoxide radicals into hydrogen peroxide and oxygen (Carvalho et al., 2015; Ye et al., 2023). For example, in cc177, the upregulation of this enzyme could be linked to its relatively low MDA content, particularly given the absence of a non-enzymatic antioxidant response. In addition, the highest increase in SOD was recorded in cc125, which exhibited strong induction of total antioxidant power and total phenolic compounds. This shows a high antioxidant defence, resulting in an intermediate increase in MDA content compared to the control. Cc114 also showed a similar variation in MDA, exhibiting strong flavonoid accumulation and high basal antioxidant capacity.

5. Conclusion

Taking into account physiological parameters, the quantification of stress-related proteins, soluble sugars, antioxidant metabolites, and MDA content illustrates the drought adaptation mechanisms of the evaluated grapevine rootstocks. The cc125 and cc114 genotypes exhibited a favourable biochemical response, strongly inducing SOD, HSP70, SuSy, soluble sugars, total antioxidant capacity, and phenolic compounds in order to cope with oxidative stress. However, they exhibited different physiological strategies, giving the former a better WUE_i. On the other hand, despite its conservative metabolism, 161.49-C is able to maintain low lipid peroxidation and basal gas exchange, resulting in a good responsive performance under drought stress. Although cc177 also maintained low MDA levels and limited metabolic adjustment, this was associated with reduced gas exchange. These findings suggest a conservative drought-avoidance strategy rather than high functional tolerance. Finally, Dog Ridge and cc136 exhibited relatively high photosynthetic activity. However, sugar depletion in the former and a reduction in SOD and HSP70 in the latter, coupled with elevated MDA levels in both, suggest an inefficient integration of osmotic and antioxidant responses, rendering them vulnerable to oxidative damage during prolonged drought.

Finally the observed physiological responses reflect short-term survival mechanisms that may not correlate with long-term biomass accumulation. Consequently, classifying genotype plasticity requires caution until supported by growth data and molecular profiling. While this study provides a robust physiological framework, a key limitation is the lack of agronomic validation. The next phase of this research program will involve grafting trials to assess scion-rootstock compatibility and verify whether the identified resilience traits persist in grafted combinations, thereby determining their actual suitability for agricultural application.

Uncited references

Gautier et al., 2020; Harris et al., 2023; Iacono et al., 1998; Marín et al., 2022; Paranychianakis et al., 2004; Peccoux et al., 2018; Wang et al., 2021; Zhao et al., 2022.

CRediT authorship contribution statement

Sara Anichini: Writing – review & editing, Writing – original draft, Methodology, Investigation, Conceptualization. **Giampiero Cai:** Writing – review & editing, Supervision, Conceptualization. **Tommaso Betti:** Writing – original draft, Methodology, Investigation. **Marco Romi:** Writing – review & editing, Supervision, Conceptualization. **Davide Bianchi:** Writing – review & editing, Resources, Conceptualization. **Lucio Brancadoro:** Writing – review & editing, Resources, Conceptualization. **Sara Parri:** Writing – review & editing, Writing – original draft, Methodology, Investigation, Conceptualization.

Declaration of competing interest

The authors declare that they have no known competing financial interests or personal relationships that could have appeared to influence the work reported in this paper.

Acknowledgements

The authors gratefully acknowledge the Santa Chiara Lab of the University of Siena, Italy (https://santachiaralab.unisi.it/), and in particular Prof. Angelo Riccaboni and Dr. Cristiana Tozzi, for providing access to the Microcosmo equipment within the Farming Lab. We would also like to thank Prof. Silvia Casini and her group at the Department of Physical, Environmental and Earth Sciences at the University of Siena for granting us access to the microplate reader used for the colorimetric assays. This equipment was acquired through the Metrofood Italia project (https://www.metrofood.it/).

Data availability

Data will be made available on request.

References

Ali, S., Mir, R.A., Haque, M.A., Danishuddin Almalki, M.A., Alfredan, M., Khalifa, A., Mahmoudi, H., Shahid, M., Tyagi, A., Mir, Z.A., 2025. Exploring physiological and molecular dynamics of drought stress responses in plants: challenges and future directions. Front. Plant Sci. 16. https://doi.org/10.3389/fpls.2025.1565635.

Amor, Y., Haigler, C.H., Johnson, S., Wainscott, M., Delmer, D.P., 1995. A membrane-associated form of sucrose synthase and its potential role in synthesis of cellulose and callose in plants. Proc. Natl. Acad. Sci. SA 92 (20), 9353–9357. https://doi.org/10.1073/pnas.92.20.9353.

Azri, W., Cosette, P., Guillou, C., Rabhi, M., Nasr, Z., Mliki, A., 2020. Physiological and proteomic responses to drought stress in leaves of two wild grapevines (*Vitis sylvestris*): a comparative study. Plant Growth Regul. 91 (1), 37–52. https://doi.org/10.1007/s10725-020-00586-4.

Bianchi, D., Brancadoro, L., 2021. Water use efficiency and nutritional status of a new grapevine rootstock selection. Horticulturae 7 (11), 503. https://doi.org/10.3390/horticulturae7110503.

Bianchi, D., Caramanico, L., Grossi, D., Brancadoro, L., De Lorenzis, G., 2020. How do novel m-rootstock (*Vitis* spp.) genotypes cope with drought? Plants 9 (10), 1385. https://doi.org/10.3390/plants9101385.

Bianchi, D., Grossi, D., Tincani, D.T., Di Lorenzo, G.S., Brancadoro, L., Rustioni, L., 2018. Multi-parameter characterization of water stress tolerance in *Vitis* hybrids for new rootstock selection. Plant Physiol. Biochem. 132, 333–340. https://doi.org/10.1016/j.plaphy.2018.09.018.

Bianchi, D., Ricciardi, V., Pozzoli, C., Grossi, D., Caramanico, L., Pindo, M., Stefani, E., Cestaro, A., Brancadoro, L., De Lorenzis, G., 2023. Physiological and transcriptomic evaluation of drought effect on own-rooted and grafted grapevine rootstock (1103P and 101-14MGt). Plants 12 (5), 1080. https://doi.org/10.3390/plants12051080.

Benzie, I.F., Strain, J.J., 1996. The ferric reducing ability of plasma (FRAP) as a measure of "antioxidant power": the FRAP assay. Anal. Biochem. 239 (1), 70–76.

Carvalho, L.C., Vidigal, P., Amâncio, S., 2015. Oxidative stress homeostasis in grapevine (*Vitis vinifera* L.). Front. Environ. Sci. 3. https://doi.org/10.3389/fenvs.2015.00020.

Cogato, A., Jewan, S.Y.Y., Wu, L., Marinello, F., Meggio, F., Sivilotti, P., Sozzi, M., Pagay, V., 2022. Water stress impacts on grapevines (*Vitis vinifera* L.) in hot environments: physiological and spectral responses. Agronomy 12 (8), 1819. https://doi.org/10.3390/agronomy12081819.

Corso, M., Vannozzi, A., Maza, E., Vitulo, N., Meggio, F., Pitacco, A., Telatin, A., D'Angelo, M., Feltrin, E., Negri, A.S., Prinsi, B., Valle, G., Ramina, A., Bouzayen, M., Bonghi, C., Lucchin, M., 2015. Comprehensive transcript profiling of two grapevine rootstock genotypes contrasting in drought susceptibility links the phenylpropanoid path-

way to enhanced tolerance. J. Exp. Bot. 66 (19), 5739–5752. https://doi.org/10.1093/jxb/erv274.
Cuena-Lombraña, A., Lallai, A., Belhadj, F., Gharbi, B., Bacchetta, G., 2022. Carignan grape cultivar salt tolerance during the germination phase across the Mediterranean basin. Seeds 1 (2), 136–145.
Dattola, A., Iuzzolini, P., Giglio Verga, F., Zappia, R., Gullo, G., 2026. Hydraulic efficiency, root allocation, and photosynthetic regulation in young grapevine rootstocks under controlled conditions. Horticulturae 12 (2), 142. https://doi.org/10.3390/horticulturae12020142.
Degu, A., Hochberg, U., Wong, D.C.J., Alberti, G., Lazarovitch, N., Peterlunger, E., Castellarin, S.D., Herrera, J.C., Fait, A., 2019. Swift metabolite changes and leaf shedding are milestones in the acclimation process of grapevine under prolonged water stress. BMC Plant Biol 19 (1). https://doi.org/10.1186/s12870-019-1652-y.
Flor, L., Toro, G., Carriquí, M., Buesa, I., Sabater, A., Medrano, H., Escalona, J.M., 2025. Impact of severe water stress on drought resistance mechanisms and hydraulic vulnerability segmentation in grapevine: the role of rootstock. J. Exp. Bot. 76 (11), 3141–3157. https://doi.org/10.1093/jxb/eraf044.
Galaz, A., Pérez-Donoso, A.G., Gambardella, M., 2024. Leaf aquaporin expression in grafted plants and the influence of genotypes and Scion/rootstock combinations on stomatal behavior in grapevines under water deficit. Plants 13 (23), 3427. https://doi.org/10.3390/plants13233427.
Galbignani, M., Merli, M.C., Magnanini, E., Bernizzoni, F., Talaverano, I., Gatti, M., Tombesi, S., Palliotti, A., Poni, S., 2016. Gas exchange and water-use efficiency of cv. Sangiovese grafted to rootstocks of varying water-deficit tolerance. Irrig. Sci. 34 (2), 105–116. https://doi.org/10.1007/s00271-016-0490-z.
Gautier, A., Cookson, S.J., Lagalle, L., Ollat, N., Marguerit, E., 2020. Influence of the three main genetic backgrounds of grapevine rootstocks on petiolar nutrient concentrations of the scion, with a focus on phosphorus. OENO One 54 (1), 1–13. https://doi.org/10.20870/oeno-one.2020.54.1.2458.
Gilbert, M.E., Pou, A., Zwieniecki, M.A., Holbrook, N.M., 2012. On measuring the response of mesophyll conductance to carbon dioxide with the variable J method. J. Exp. Bot. 63 (1), 413–425. https://doi.org/10.1093/jxb/err288.
Guo, Y., Li, S., García-Caparros, P., Wang, L., Liang, Z., 2025. Grapevine adaptation to cold and heat stress. J. Exp. Bot. 76 (11), 3038–3058. https://doi.org/10.1093/jxb/eraf158.
Gutiérrez-Gamboa, G., Pérez-Donoso, A.G., Pou-Mir, A., Acevedo-Opazo, C., Valdés-Góme, H., 2019. Hydric behaviour and gas exchange in different grapevine varieties (*Vitis vinifera* L.) from the Maule Valley (Chile). S. Afr. J. Enol. Vitic. 40 (2), 1. https://doi.org/10.21548/42-2-3224, 1.
Haider, M.S., Zhang, C., Kurjogi, M.M., Pervaiz, T., Zheng, T., Zhang, C., Lide, C., Shangguan, L., Fang, J., 2017. Insights into grapevine defense response against drought as revealed by biochemical, physiological and RNA-seq analysis. Sci. Rep. 7 (1), 13134. https://doi.org/10.1038/s41598-017-13464-3.
Harris, Z.N., Pratt, J.E., Kovacs, L.G., Klein, L.L., Kwasniewski, M.T., Londo, J.P., Wu, A.S., Miller, A.J., 2023. Grapevine scion gene expression is driven by rootstock and environment interaction. BMC Plant Biol. 23 (1), 211. https://doi.org/10.1186/s12870-023-04223-w.
Hodges, D.M., DeLong, J.M., Forney, C.F., Prange, R.K., 1999. Improving the thiobarbituric acid-reactive-substances assay for estimating lipid peroxidation in plant tissues containing anthocyanin and other interfering compounds. Planta 207 (4), 604–611. https://doi.org/10.1007/s004250050524.
Iacono, F., Buccella, A., Peterlunger, E., 1998. Water stress and rootstock influence on leaf gas exchange of grafted and ungrafted grapevines. Sci. Hortic. 75 (1–2), 27–39. https://doi.org/10.1016/S0304-4238(98)00113-7.
Ismail, A., Gajjar, P., Darwish, A.G., Abuslima, E., Islam, T., Mohamed, A.G., El-Sharkawy, I., 2025. Redox and osmotic homeostasis: central drivers of drought resilience in grapevine rootstocks. Plant Physiol. Biochem. 221, 109618. https://doi.org/10.1016/j.plaphy.2025.109618.
Jiao, S., Zeng, F., Huang, Y., Zhang, L., Mao, J., Chen, B., 2023. Physiological, biochemical and molecular responses associated with drought tolerance in grafted grapevine. BMC Plant Biol 23 (1). https://doi.org/10.1186/s12870-023-04109-x.
Jones, G.V., Edwards, E.J., Bonada, M., Sadras, V.O., Krstic, M.P., Herderich, M.J., 2022. 17—Climate change and its consequences for viticulture. In: Reynolds, A.G. (Ed.), Managing Wine Quality, Second Edition. Woodhead Publishing, pp. 727–778. https://doi.org/10.1016/B978-0-08-102067-8.00015-4.
Ju, Y., Min, Z., Zhang, Y., Zhang, K., Liu, M., Fang, Y., 2021. Transcriptome profiling provides new insights into the molecular mechanism of grapevine response to heat, drought, and combined stress. Sci. Hortic. 286, 110076. https://doi.org/10.1016/j.scienta.2021.110076.
Keller, M., 2010. Managing grapevines to optimise fruit development in a challenging environment: a climate change primer for viticulturists. Aust. J. Grape Wine Res. 16, 56–69. https://doi.org/10.1111/j.1755-0238.2009.00077.x.
Khadka, V.S., Vaughn, K., Xie, J., Swaminathan, P., Ma, Q., Cramer, G.R., Fennell, A.Y., 2019. Transcriptomic response is more sensitive to water deficit in shoots than roots of *Vitis riparia* (Michx.). BMC Plant Biol. 19 (1), 72. https://doi.org/10.1186/s12870-019-1664-7.
Koc, M., Cangi, R., Yildiz, K., 2023. Effect of drought on aquaporin expression in grafted and ungrafted grapevine cultivars. Ciência Téc. Vitiv. 38 (1), 35–42. https://doi.org/10.1051/ctv/ctv20233801035.
Koundouras, S., Tsialtas, I.T., Zioziou, E., Nikolaou, N., 2008. Rootstock effects on the adaptive strategies of grapevine (*Vitis vinifera* L. cv. Cabernet–Sauvignon) under contrasting water status: leaf physiological and structural responses. Agric. Ecosyst. Environ. 128 (1–2), 86–96. https://doi.org/10.1016/j.agee.2008.05.006.
Krishankumar, S., Hunter, J.J., Alyafei, M., Souka, U., Subramaniam, S., Ramlal, A., Kurup, S.S., Amiri, K.M.A., 2025. Influence of different scion-rootstock combinations on sugars, polyamines, antioxidants and malondialdehyde in grafted grapevines under arid conditions. Front. Plant Sci. 16, 1559095. https://doi.org/10.3389/fpls.2025.1559095.
Labarga, D., Mairata, A., Puelles, M., Martín, I., Albacete, A., García-Escudero, E., Pou, A., 2023. The rootstock genotypes determine drought tolerance by regulating aquaporin expression at the transcript level and phytohormone balance. Plants 12 (4), 718. https://doi.org/10.3390/plants12040718.
Li, J., Hu, Y., Hu, J., Xie, Q., Chen, X., Qi, X., 2024. Sucrose synthase: an enzyme with multiple roles in plant physiology. J. Plant Physiol. 303, 154352. https://doi.org/10.1016/j.jplph.2024.154352.
Lin, Y., Liu, S., Fang, X., Ren, Y., You, Z., Xia, J., Hakeem, A., Yang, Y., Wang, L., Fang, J., Shangguan, L., 2023. The physiology of drought stress in two grapevine cultivars: photosynthesis, antioxidant system, and osmotic regulation responses. Physiol. Plant. 175 (5). https://doi.org/10.1111/ppl.14005.
Liu, X., Chen, H., Li, S., Wang, L., 2022. Genome-wide identification of the Hsp70 gene Family in grape and their expression profile during. Abiotic Stress. Horticulturae 8 (8), 743. https://doi.org/10.3390/horticulturae8080743.
Lucini, L., Miras-Moreno, B., Busconi, M., Marocco, A., Gatti, M., Poni, S., 2020. Molecular basis of rootstock-related tolerance to water deficit in *Vitis vinifera* L. cv. Sangiovese: a physiological and metabolomic combined approach. Plant Sci. 299, 110600. https://doi.org/10.1016/j.plantsci.2020.110600.
Marguerit, E., Brendel, O., Lebon, E., Van Leeuwen, C., Ollat, N., 2012. Rootstock control of scion transpiration and its acclimation to water deficit are controlled by different genes. New Phytol. 194 (2), 416–429. https://doi.org/10.1111/j.1469-8137.2012.04059.x.
Marín, D., Torres, N., Dayer, S., Villa-Llop, A., Abad, F.J., Gambetta, G.A., Inta, E., 2022. Effects of graft quality on growth and grapevine-water relations. InTerClim 2022-14. International Terroir Congress.
Marusig, D., Tombesi, S., 2020. Abscisic acid mediates drought and salt stress responses in *Vitis vinifera* - a review. Int. J. Mol. Sci. 21 (22), 8648. https://doi.org/10.3390/ijms21228648.
Maurel, C., Boursiac, Y., Luu, D.T., Santoni, V., Shahzad, Z., Verdoucq, L., 2015. Aquaporins in plants. Physiol. Rev. 95, 1321–1358. https://doi.org/10.1152/physrev.00008.2015.
Meggio, F., Prinsi, B., Negri, A.S., Simone Di Lorenzo, G., Lucchini, G., Pitacco, A., Failla, O., Scienza, A., Cocucci, M., Espen, L., 2014. Biochemical and physiological responses of two grapevine rootstock genotypes to drought and salt treatments: response of two genotypes to drought and salinity. Aust. J. Grape Wine Res. 20 (2), 310–323. https://doi.org/10.1111/ajgw.12071.
Merli, M.C., Magnanini, E., Gatti, M., Pirez, F.J., Pueyo, I.B., Intrigliolo, D.S., Poni, S., 2016. Water stress improves whole-canopy water use efficiency and berry composition of cv. Sangiovese (*Vitis vinifera* L.) grapevines grafted on the new drought-tolerant rootstock M4. Agric. Water Manag. 169, 106–114. https://doi.org/10.1016/j.agwat.2016.02.025.
Migliaro, D., De Lorenzis, G., Di Lorenzo, G.S., De Nardi, B., Gardiman, M., Failla, O., Brancadoro, L., Crespan, M., 2019. Grapevine non-vinifera genetic diversity assessed by simple sequence repeat markers as a starting point for new rootstock breeding programs. Am. J. Enol. Vitic. 70 (4), 390–397. https://doi.org/10.5344/ajev.2019.18054.
Morales, M., Munné-Bosch, S., 2019. Malondialdehyde: facts and artifacts. Plant Physiol. 180 (3), 1246–1250. https://doi.org/10.1104/pp.19.00405.
Nazir, F., Ahmad, T., Malik, S.I., Ahmed, M., Bashir, M.A., 2022. Wild grapevines as rootstock regulate the oxidative defense system of in vitro grafted scion varieties under drought stress. PLoS ONE 17 (9), e0274387. https://doi.org/10.1371/journal.pone.0274387.
Ozturk, M., Turkyilmaz Unal, B., García-Caparrós, P., Khursheed, A., Gul, A., Hasanuzzaman, M., 2021. Osmoregulation and its actions during the drought stress in plants. Physiol. Plant. 172 (2), 1321–1335. https://doi.org/10.1111/ppl.13297.
Paranychianakis, N.V., Aggelides, S., Angelakis, A.N., 2004. Influence of rootstock, irrigation level and recycled water on growth and yield of Soultanina grapevines. Agric. Water Manag. 69 (1), 13–27. https://doi.org/10.1016/j.agwat.2004.03.012.
Parri, S., Faleri, C., Romi, M., Del Río, J.C., Rencoret, J., Dias, M.C.P., Anichini, S., Cantini, C., Cai, G., 2024. Unravelling different water management strategies in three olive cultivars: the role of osmoprotectants, proteins, and wood properties. Int. J. Mol. Sci. 25 (20), 11059. https://doi.org/10.3390/ijms252011059.
Peccoux, A., Loveys, B., Zhu, J., Gambetta, G.A., Delrot, S., Vivin, P., Schultz, H.R., Ollat, N., Dai, Z., 2018. Dissecting the rootstock control of scion transpiration using model-assisted analyses in grapevine. Tree Physiol. 38 (7), 1026–1040. https://doi.org/10.1093/treephys/tpx153.
Pou, A., Medrano, H., Flexas, J., Tyerman, S.D., 2013. A putative role for TIP and PIP aquaporins in dynamics of leaf hydraulic and stomatal conductances in grapevine under water stress and re-watering. Plant Cell Environ. 36 (4), 828–843. https://doi.org/10.1111/pce.12019.
Prinsi, B., Negri, A.S., Failla, O., Scienza, A., Espen, L., 2018. Root proteomic and metabolic analyses reveal specific responses to drought stress in differently tolerant grapevine rootstocks. BMC Plant Biol. 18 (1), 126. https://doi.org/10.1186/s12870-018-1343-0.
Prinsi, B., Simeoni, F., Galbiati, M., Meggio, F., Tonelli, C., Scienza, A., Espen, L., 2021. Grapevine rootstocks differently affect physiological and molecular responses of the scion under water deficit condition. Agronomy 11 (2), 289. https://doi.org/10.3390/agronomy11020289.
Rius-Garcia, X., Videgain-Marco, M., Casanova-Gascón, J., Acuña-Rello, L., Martín-Ramos, P., 2025. Physiological response to salinity in novel M-series grapevine rootstocks: a comparison with commercial standards. Agronomy 15 (2), 473.
Rogiers, S.Y., Greer, D.H., Liu, Y., Baby, T., Xiao, Z., 2022. Impact of climate change on grape berry ripening: an assessment of adaptation strategies for the Australian vineyard. Front. Plant Sci. 13. https://doi.org/10.3389/fpls.2022.1094633.

Romero, P., Botía, P., Morote, E.I., Morte, A., Navarro, J.M., 2025. Microbial inoculation differentially affected the performance of field-grown young monastrell grapevines under semiarid conditions. Depending Rootstock. Agron. 15 (11), 2570. https://doi.org/10.3390/agronomy15112570.

Sabir, F., Zarrouk, O., Noronha, H., Loureiro-Dias, M.C., Soveral, G., Gerós, H., Prista, C., 2021. Grapevine aquaporins: diversity, cellular functions, and ecophysiological perspectives. Biochimie 188, 61–76. https://doi.org/10.1016/j.biochi.2021.06.004.

Savic, S., Petranovic, N., Trmčić, S., Grujić, O., Cindric, P., Krstov, D., 2004. Influence of the clone 114 from b x r kober 5bb rootstock on the grapevine quality and yield of the italian riesling grown at the Vršac vineyard region. Acta Hortic (652), 223–231. https://doi.org/10.17660/ActaHortic.2004.652.28.

Scholasch, T., Rienth, M., 2019. Review of water deficit mediated changes in vine and berry physiology: consequences for the optimization of irrigation strategies. OENO One 53. https://doi.org/10.20870/oeno-one.2019.53.3.2329.

Schultz, H.R., Stoll, M., 2010. Some critical issues in environmental physiology of grapevines: future challenges and current limitations. Aust. J. Grape Wine Res. 16, 4–24. https://doi.org/10.1111/j.1755-0238.2009.00074.x.

Serra, I., Strever, A., Myburgh, P.A., Deloire, A., 2014. Review: the interaction between rootstocks and cultivars (*Vitis vinifera* L.) to enhance drought tolerance in grapevine: rootstocks to enhance drought tolerance in grapevine. Aust. J. Grape Wine Res. 20 (1), 1–14. https://doi.org/10.1111/ajgw.12054.

Singh, M., Kumar, J., Singh, S., Singh, V.P., Prasad, S.M., 2015. Roles of osmoprotectants in improving salinity and drought tolerance in plants: a review. Rev. Environ. Sci. Bio/Technol. 14 (3), 407–426. https://doi.org/10.1007/s11157-015-9372-8.

Singleton, V.L., Rossi, J.A., 1965. Colorimetry of total phenolics with phosphomolybdic-phosphotungstic acid reagents. Am. J. Enol. Vitic. 16 (3), 144–158.

Smirnova, L.P., Pervykh, L.N., 1998. Quantitative determination of the total content of flavonoids in the flowers of immortelle *Helichrysum arenarium*. Pharm. Chem. J. 32 (6), 321–324. https://doi.org/10.1007/BF02580519.

Sucu, S., Yağcı, A., Yıldırım, K., 2018. Changes in morphological, physiological traits and enzyme activity of grafted and ungrafted grapevine rootstocks under drought stress. Erwerbs-Obstbau 60 (2), 127–136. https://doi.org/10.1007/s10341-017-0345-7.

Tomás, M., Medrano, H., Escalona, J.M., Martorell, S., Pou, A., Ribas-Carbó, M., Flexas, J., 2014. Variability of water use efficiency in grapevines. Environ. Exp. Bot. 103, 148–157. https://doi.org/10.1016/j.envexpbot.2013.09.003.

Van Leeuwen, C., Destrac-Irvine, A., Dubernet, M., Duchêne, E., Gowdy, M., Marguerit, E., Pieri, P., Parker, A., De Rességuier, L., Ollat, N., 2019. An update on the impact of climate change in viticulture and potential adaptations. Agronomy 9 (9), 514. https://doi.org/10.3390/agronomy9090514.

Vandeleur, R.K., Mayo, G., Shelden, M.C., Gilliham, M., Kaiser, B.N., Tyerman, S.D., 2009. The role of plasma membrane intrinsic protein aquaporins in water transport through roots: diurnal and drought stress responses reveal different strategies between isohydric and anisohydric cultivars of grapevine. Plant Physiol. 149 (1), 445–460. https://doi.org/10.1104/pp.108.128645.

Venios, X., Korkas, E., Nisiotou, A., Banilas, G., 2020. Grapevine responses to heat stress and global warming. Plants 9 (12), 1754. https://doi.org/10.3390/plants9121754.

Wang, X., Yan, L., Wang, B., Qian, Y., Wang, Z., Wu, W., 2021. Comparative proteomic analysis of grapevine rootstock in response to waterlogging stress. Front. Plant Sci. 12, 749184. https://doi.org/10.3389/fpls.2021.749184.

Waters, E.R., Lee, G.J., Vierling, E., 1996. Evolution, structure and function of the small heat shock proteins in plants. J. Exp. Bot. 47 (3), 325–338. https://doi.org/10.1093/jxb/47.3.325.

Wu, X., Xiong, E., Wang, W., Scali, M., Cresti, M., 2014. Universal sample preparation method integrating trichloroacetic acid/acetone precipitation with phenol extraction for crop proteomic analysis. Nat. Protoc. 9 (2), 362–374. https://doi.org/10.1038/nprot.2014.022.

Ye, Q., Wang, H., Li, H., 2023. Arbuscular mycorrhizal fungi enhance drought stress tolerance by regulating osmotic balance, the antioxidant system, and the expression of drought-responsive genes in Vitis vinifera L. Aust. J. Grape Wine Res. 2023, 1–13. https://doi.org/10.1155/2023/7208341.

Yıldırım, K., Yağcı, A., Sucu, S., Tunç, S., 2018. Responses of grapevine rootstocks to drought through altered root system architecture and root transcriptomic regulations. Plant Physiol. Biochem. 127, 256–268. https://doi.org/10.1016/j.plaphy.2018.03.034.

Zhao, F., Zheng, T., Liu, Z., Fu, W., Fang, J., 2022. Transcriptomic analysis elaborates the resistance mechanism of grapevine rootstocks against salt stress. Plants 11 (9), 1167. https://doi.org/10.3390/plants11091167.

Zivcak, M., Brestic, M., Sytar, O., 2016. Osmotic adjustment and plant adaptation to drought stress. In: Drought Stress Tolerance in Plants, 1. Springer International Publishing, pp. 105–143. https://doi.org/10.1007/978-3-319-28899-4_5.